

Investigating the antimalarial properties of small-molecule compounds and exploring
Plasmodium falciparum hexokinase as a potential therapeutic target

Undergraduate Research Thesis

Presented in Partial Fulfillment of the Requirements for graduation with “Honors Research
Distinction in Biochemistry” in the college of Honors Arts & Science at The Ohio State
University

May 2020

By

Abu Rogers

From

Freetown, Sierra Leone

Project Advisors: Mark E. Drew, Ph.D., Department of Microbial Infection and Immunity

Jane E. Jackman, Ph.D., Department of Biochemistry and Chemistry

Summary

Malaria, a deadly tropical disease transmitted by infected mosquitos, is caused by *Plasmodium* parasites. *Plasmodium falciparum* is the most pathogenic form, responsible for >95% of mortality. Continual development of therapeutic drug resistance necessitates the search for novel antimalarial therapeutics.

In an aim to find novel anti-malarial therapeutics, the five small-molecule compounds were screened for their ability to kill *P. falciparum* parasites. The compounds were purified from *Cinnamosma fragrans*, a plant endemic to Madagascar commonly used as an antimalaria treatment. A 72-hour dose response assay was performed with the asexual stages of the parasite, and the percent inhibition of each drug was determined relative to the negative DMSO-control. CMOS was the most potent with an IC₅₀ of 0.4148 micromolar, followed by CM18 with an IC₅₀ of 0.9858 micromolar.

In a target-based approach, this second part of the project focuses on characterizing the biochemical properties of *P. falciparum* hexokinase (PfHK) and studying how its properties change through the intra-erythrocytic life stages of *P. falciparum*. The parasite's single hexokinase enzyme is solely responsible for the conversion of glucose to glucose-6-phosphate, the necessary substrate for production of ATP via glycolysis or generation of reducing equivalents (NADPH) and ribose-5-phosphate via the pentose phosphate pathway. Glycolytic flux in the parasite has been shown to be regulated during the parasite's pathogenic, erythrocytic stages, with PfHK activity being suggested as the rate-limiting step. We are exploring the idea that regulated post-translational modification of PfHK and/or turnover is responsible for its catalytic activity. To test this hypothesis, polyclonal antisera was generated, which specifically

recognizes PfHK. Western blotting of *P. falciparum* whole-cell lysate, under reducing conditions, recognizes a single band of ~55 kDa as is predicted. However, under native conditions, a single band of ~220 kDa is detected, suggestive of PfHK forming a homotetramer *in vivo*, which has not been described for other eukaryotic HKs. Recently published structural studies of recombinant PvHK in the Morris lab supports this observation (1). Furthermore, using our PfHK antisera we have successfully immunopurified the protein from the parasite and are in process of identifying post-translational modifications and possible binding partners.

Immunofluorescence assays (IFA) were also performed to determine the location and expression of PfHk in the different life stages. Results from the IFA support previous hypotheses that the enzyme is cytosolic and is expressed in all stages. Additionally, SeaHorse XF and kinetic assays were performed to determine how the glycolytic flux and the activity of PfHk changes through the life cycle of the parasite, respectively. The results from the kinetic experiments show that trophozoites have the highest HK content with the lowest turnover rate; whereas the gametocytes had unmeasurable PfHk activity. The SeaHorse XF assays also showed that the asexual stages had measurable glycolytic flux relative to the sexual stages, which had a very low glycolytic flux. Thus, even though HK is expressed in the matured sexual stages, it is not active. Therefore, unraveling the mechanism by which PfHk activity is regulated in sexual stages is a promising next step to understanding how PfHk could be targeted in novel antimalarial therapeutics.

Acknowledgement

I am immensely grateful for the guidance of my project advisor, Dr. Drew. His excellent mentorship has not only nurtured my interests in biomedical research, but it also encouraged me to complete my major in Biochemistry at the Ohio State University despite all the adversities. I am forever indebted to the skills, lessons, and resources he has provided me with. My undergraduate career and aspirations to be a physician-investigator would not have been possible without his help. I would also like to thank current and previous members associated with the Drew Lab, especially Najmus Mahfooz, Hema Kasinathan, and Maria Barreras, for the supportive environment, kindness, and help they provided.

I would like to thank our collaborators, Dr. James Morris and Dr. Liva Rakotondraibe for providing the *Plasmodium vivax* hexokinase and the *Cinnamosma frangnans* compounds, respectively.

I am grateful for Dr. Jane Jackman for being my Biochemistry advisor, professor, and a part of my defense committee. I would also like to thank Dr. Jesse Kwiek for serving on my thesis committee.

I would like to thank the Undergraduate Research Office, the Department of Biochemistry & Chemistry, and the Honors Arts & Sciences for their generosity in research grants and scholarships. Thanks to the Microbial Infections & Immunity Department for providing the resources that made this project possible.

Table of Contents

Summary.....	2
Acknowledgement.....	4
List of tables and figures.....	6
Chapter 1. Background.....	7
1.1. Introduction.....	7
1.2. Life cycle.....	7
1.3. Malaria drug resistance.....	8
Chapter 2. Investigating the antimalarial properties of purified compounds from <i>C. fragrans</i> ...	10
2.1. Introduction.....	10
2.1.1. Origin and properties of <i>C. fragrans</i>	10
2.1.2. Therapeutic development.....	10
2.2. Methods and materials.....	11
2.2.1. <i>In vitro</i> parasite culture.....	11
2.2.2. <i>In vitro</i> dose response assay.....	12
2.3. Results.....	13
2.4. Discussion.....	16
Chapter 3. Validating PfHk as a potential therapeutic target.....	17
3.1: Introduction.....	17
3.1.1. Biochemistry of hexokinase.....	17
3.1.2. Glucose metabolism.....	18
3.1.3. Life stages and metabolic properties.....	19
3.1.4. Post-translational modifications in PfHk.....	20
3.2: Materials and methods.....	21
3.2.1. Synchronization, harvest, and lysate preparation.....	21
3.2.2. PfHk antiserum production.....	22
3.2.3. Recombinant PvHk generation.....	22
3.2.4. SeaHorse XF assay.....	22
3.2.5. Kinetic assay.....	23
3.2.6. Western blot.....	25
3.2.7. Estimating the protein concentration.....	26
3.2.8. Immunoprecipitation and proteomic analysis.....	27
3.2.9. Immunofluorescence assay.....	27
3.3: Results.....	28
3.3.1. Matured sexual stages are glycolytically inactive.....	28
3.3.2. Expression and cellular localization of PfHk.....	29
3.3.3. Biochemical properties of PfHk parasite.....	30
3.3.4. PfHk is a tetramer <i>in vivo</i>	33
3.3.5. Immunoprecipitation.....	35
3.4: Discussion.....	36
References.....	40

List of figures

- [Figure 1](#): Life cycle of *Plasmodium falciparum*
[Figure 2](#): Life stages versus time post-invasion
[Figure 3](#): Non-linear regression curves of compounds extracted from *Cinnamosma fragrans*
[Figure 4](#): Methodology flowchart
[Figure 5](#): Fate of glucose 6-phosphate
[Figure 6](#): Alignments of PfHk, PvHk, and human glucokinase
[Figure 7](#): NADP-coupled kinetic assay
[Figure 8](#): Seahorse XF assays for asexual and sexual stages
 8a: Extracellular acidification rate for asexual and sexual
 8b: Extracellular acidification rate for the sexual stages
[Figure 9](#): Immunofluorescence assays for the asexual stages
[Figure 10](#): Immunofluorescence assays for the sexual stages
[Figure 11](#): Protein content for rings, trophozoites, schizonts.
[Figure 12](#): Substrate curve and double-reciprocal plots for the stage-specific harvests
[Figure 13](#): Activity of PfHk through the lifecycle of the parasite
[Figure 14](#): Western blots for the asexual and sexual stages in native and reducing conditions
[Figure 15](#): Western blot and silver staining for immunoprecipitation

List of tables

- [Table 1](#): Past and current antimalarial treatments
[Table 2](#): *Cinnamosma fragrans* compound structures and IC₅₀
[Table 3](#): Percent of protein in rings, trophozoites, and schizonts
[Table 4](#): K_m and K_{cat} of PfHK and copies of PfHk per parasite

Chapter 1: Background

1.1 Introduction

Malaria is a deadly infectious disease caused by the *Plasmodium* parasites and transmitted by the female *Anopheles* mosquito. In 2018, there were 228 million cases worldwide, with 213 million affecting Africa, and it was responsible for 405,000 deaths (2). Thus, malaria continues to be a major burden to the countries affected.

There are five species in the *Plasmodium* genus, *P. falciparum*, *P. vivax*, *P. malariae*, *P. ovale*, and *P. knowlesii*, responsible for human malaria. *P. falciparum* and *P. vivax* are the two most common, with *P. falciparum* being the most virulent species responsible for >95% mortality (2).

1.2 Life cycle of *P. falciparum*

P. falciparum has multiple life stages within the human host: primarily the asexual blood stages, sexual blood stages, and sporozoites. The asexual blood stages cause the symptoms of the disease, and they are divided into the ring, trophozoite, and schizont stages. The sexual stages, or gametocytes, are responsible for the transmission of the disease from a human to a mosquito, and the sporozoites facilitate transmission from a mosquito to a human host.

Infection of malaria begins with a female *Anopheles* mosquito bite, which transmits sporozoites to the human's blood, through its saliva. The sporozoites then travel to the liver, where they infect hepatocytes to begin the exo-erythrocytic cycle (fig. 1). Completion of this stage results in the release of merozoites which then infect erythrocytes, thus initiating the erythrocytic phase of their development (fig. 1). When the merozoites invade an erythrocyte, they enter the ring stage, and within 24 hours, they develop into trophozoites (fig. 2).

Approximately 36 hours post-invasion, the matured trophozoites then undergo several nuclear divisions within the same cell, which is referred to as a schizont. The schizonts burst open to release up to 32 merozoites, following the completion of the life cycle at 44 hours. The merozoites then invade new red blood cells to repeat the cycle.

A small percentage of the asexual stages branch out to produce the sexual stages of the parasite. Previous studies have estimated the ratio of sexual to asexual stages to be less than 1:10 (3). This ratio is largely influenced by the environment of the host, specifically the pH, temperature, and parasitemia. Despite the small percentage of the sexual stages, they play a pivotal role in the high success rate of *P. falciparum*, as they undergo drastic changes during their development to maximize their chances of survival in the mosquito (4).

The mechanism by which sexual stages are formed, referred to as gametocytogenesis, remains unclear, but previous studies have shown that schizonts are committed to producing either the sexual or asexual stages (5) and that the sexual stages from a single schizont are either all males or females (6). After the initiation of gametocytogenesis, the parasites develop into microgametocytes (male) and macrogametocytes (females). The production of macrogametocytes is much higher than that of microgametes to account for exflagellation in the microgametocytes, which produces eight microgametes (4).

1.3 Malaria drug resistance

Artemisinin-based combination therapy (ACT), which uses artemisinin (short-acting) with a one or more long-acting, complementary compounds, has been the main form of treatment for malaria, with an estimated 3 billion treatment courses used from 2010 to 2018 (2). However, in recent years, there has been a surge in *P. falciparum* resistance to ACT, which has amplified

the impact of multi-drug resistance in the affected countries (7). If the spread of resistance surpasses the development of new therapeutics, then the advances that have been to eliminate the disease would be nullified. This necessitates the need for specific and selective drug targets and novel antimalarial therapeutics. Therefore, this study utilizes a dual approach to address resistance by finding small-molecule compounds with curative properties and understanding how PfHk could serve as a selective and specific therapeutic target.

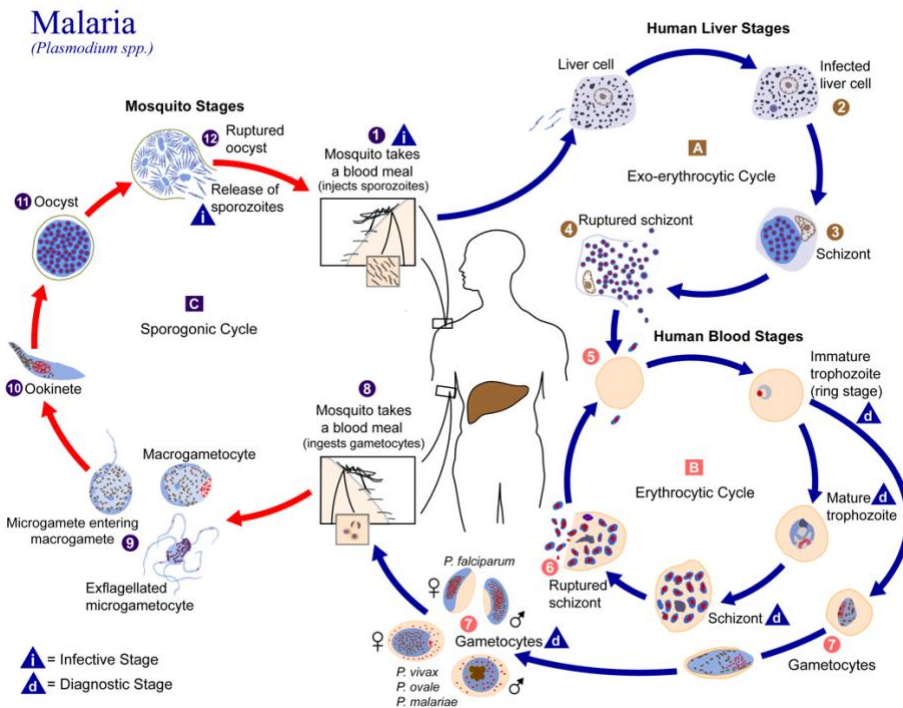


Figure 1: Life cycle of the *P. falciparum* parasite in the female *Anopheles* mosquito and humans. Image from and produced by CDC — DPDx/Alexander J. da Silva, Melanie Moser (8).

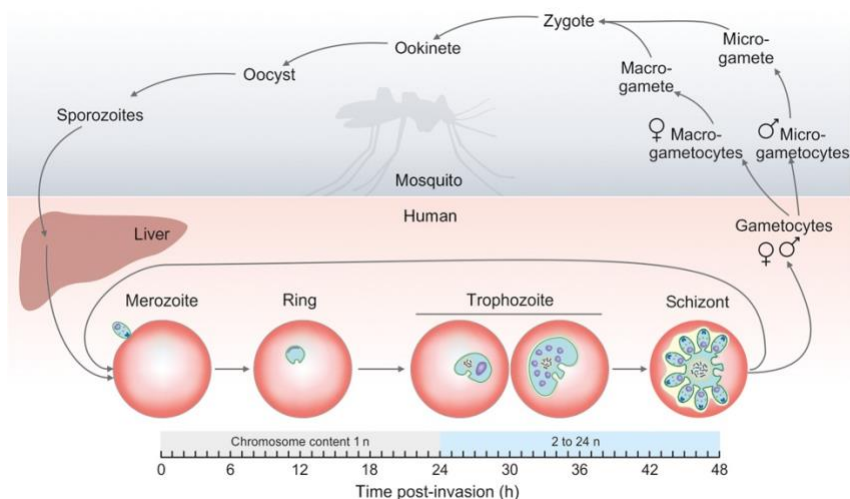


Figure 2: Life cycle of *P. falciparum* parasite that shows the different stages of the asexual form of the parasite, post-invasion (9).

Chapter 2: Investigating the antimalarial properties of compounds purified from *Cinnamosma fragrans*

2.1 Introduction

2.1.1 Origin and properties of *C. fragrans*

Three species belong to the genus *Cinnamosma* (*Cinnamosma fragrans*, *C. macrocarpa*, *C. madagascariensis*) and they are commonly used in traditional medicine as a cure for malaria, fatigue, and muscle aches (10). The bark of *C. fragrans* is rich in drimane sesquiterpenes, which contributes to its antimalarial properties (11). Cinnamodial (CDIAL), the main compound in the bark, and cinnamosmolide (CMOS) are toxic to cancer cells, have antifungal properties, and can inhibit glucosidase activity. CDIAL was isolated from the dichloromethane extracts of *C. fragrans*, and CMOS is a derivative of CDIAL with the aldehyde group substituted with a γ -lactone ring. CM18, CM18OX, UGDL are other compounds extracted from *C. fragrans*, with different modifications, that were also studied in this project.

2.1.2 Therapeutic Development

Since the 1820s, several anti-malarial therapeutics have been developed. The first chemically purified compound used to treat malaria was quinine, followed by mepacrine during the Second World War, and then chloroquine in the 1940s (12). However, due to malaria drug resistance, quinine and chloroquine are no longer used. Mepacrine use has also been stopped due to its toxicity. According to the WHO Model List that was posted in 2019, there are currently fourteen therapeutics used to cure malaria and four used as prophylaxis in patients (13). The most successful anti-malarial therapeutics are artemisinin-based combinations (12), as they have been shown to be the most effective against the multi-drug resistant forms of *P. falciparum*. Despite their success, there is still a rising concern for the development of new drug resistance in *P. falciparum*, which necessitates the search for selective and specific inhibitors of novel drug targets.

Drug	Description (year of discovery, mechanism of action, current use and resistance)	Prophylactic or curative	Origin
Quinine	Discovered in 1820. Interferes with hemoglobin digestion. Resistance was first reported in 1980s. It is no longer used as the main form of treatment. Typically used in combination with antibiotics.	Curative	Bark of cinchona tree
Chloroquine	First use for malaria was in the 1940s. It interferes with hemozoin formation and inhibits DNA and RNA biosynthesis. Resistance was reported in 1950s. Now it is only used for <i>P. vivax</i> in regions with no known resistance.	Prophylactic and Curative	Analog of quinine
Mefloquine	Developed in 1970. It disrupts hemoglobin digestion, and it is used in combination with a complementary drug. It is less commonly used due to potential effects on the Central Nervous System and drug resistance.	Prophylactic and curative	Developed by US Army

Artemisinin	First discovered in 1971, it is the major form of treatment in artemisinin-combination therapy (ACT). Some cases of resistance have been recorded. It increases reactive oxidative species and decreases parasite development. Artesunate, artemether, and arteether are common derivatives.	Curative	<i>Artemisia annua</i> , a herb used in Chinese traditional medicine
Pyrimethamine & Sulfadoxine	Pyrimethamine and Sulfadoxine were developed in the 1950s and 1960s, respectively. Both drugs are used as combination therapy and they target the folate biosynthesis pathway.	Curative	Synthesized by different entities
Mepacrine	It is derivative of methylene blue, a potent anti-malarial. No longer used due to its side effects, like toxic psychosis.	Prophylactic	Derivative of methylene blue

Table 1: A list of common past and current anti-malaria treatment, their discovery, and mechanism of action. (12)

2.2 Materials and methods

2.2.1 *In vitro* parasite culture

P. falciparum 3D7 parasites were grown in O-positive blood at 2% hematocrit and RPMI media. The media contained 0.5% AlbuMAX (Albx), 0.37 mM hypoxanthine, 27 mM NaHCO₃, 11 mM glucose, and 10 µg/ml gentamicin. All cultures were incubated at 37°C in 5% CO₂, 5% O₂, and 90% N₂ (14). The health of the parasites was analyzed using blood smears and the parasitemia was determined using flow-cytometry. The acridine orange used in flowcytometry stains the nucleic acid, and the flow-cytometry detects the percentage of red blood cells with staining. The media and blood were changed regularly, and a new batch of packed red blood cells and media were prepared every four weeks.

Gametocytogenesis Induction

Gametocytes were obtained from the *P. falciparum* 3D7 strains following the protocol used by Fiveman et. al with some modifications (15). On day 0, asexual MR4 at 2 % parasitemia were synchronized using 5% D-Sorbitol to isolate the desired ring and late-stage schizont parasites. The hematocrit was increased from the regular 2% to 3%. On day 2, the hematocrit was reduced to 2% by increasing the volume of media. From day 8-11, 50 mM N-acetyl glucosamine were added to the cultures to kill the asexual stages in the culture. Blood smears were made daily to observe the quality of the culture and the parasitemia. On day 12, the gametocytes were harvested using a 0.025% saponin, and the parasites were stored in Potassium-buffered saline (PBS) with protease inhibitors at -80°.

2.2.2 *In vitro* anti-asexual assays

The effect of five compounds on the asexual stages of *P. falciparum* 3D7 was investigated. The compounds were extracted from *C. fragrans*. The five compounds tested were CMOS, CDIAL, UGDL, CM18, and CM18OX. All compounds were dissolved in DMSO to make stock concentration for the experiments. Chloroquine served as the positive control.

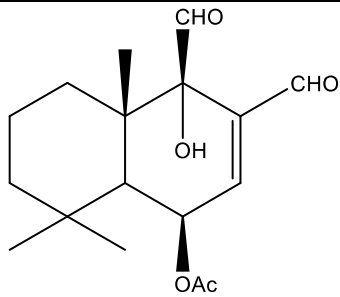
MR4 3D7 parasites were cultured using the protocol above (2.2.1), and the parasites were used for the 72-hour dose response assays. On the day of the assay, the parasitemia of healthy asynchronized cultures were determined. 100 µL of media, containing the compounds, was added to each well, and this was followed by a 10-fold serial dilution. 100 µL of cell culture (2% hematocrit and 1% parasitemia) was added to each well to bring the final volume to 200 µL (1% hematocrit and 0.5% parasitemia). The plates were then incubated at 37°C for 72 hours. After 72 hours, if the parasitemia of the negative DMSO control wells were high enough (at least 7%), the parasitemia of the all groups were then determined via flowcytometry. Thin blood smears were

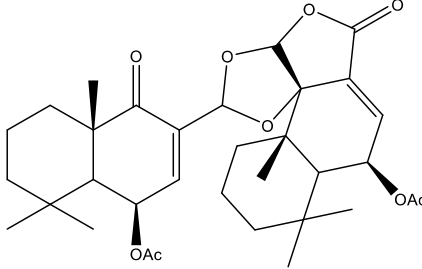
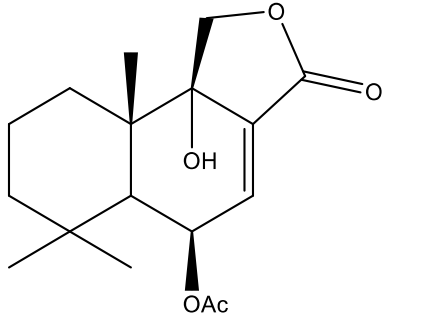
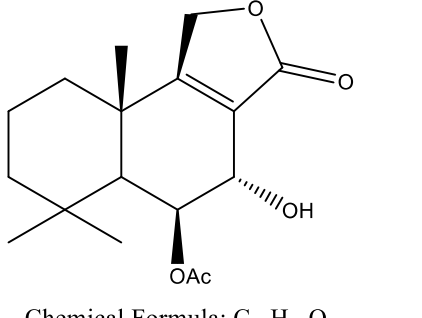
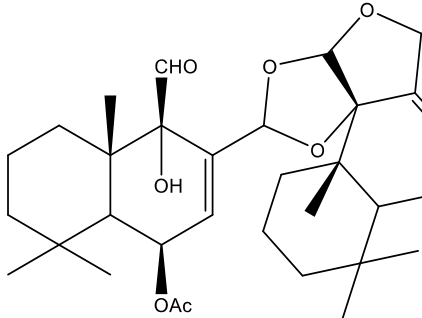
also made to assess the health of the parasites. The percent inhibition of the compounds was calculated relative to the negative DMSO-control wells.

2.3 Results

Cinnamosma fragrans: asexual dose response assays

A 72-hour dose response assay was performed to determine the antimalarial properties of five compounds extracted from *C. fragrans*. The percent inhibition of the compounds was determined by comparing the parasitemia of the treated wells with the DMSO negative control. A nonlinear regression curve was generated using Prism 8 (graph pad) to determine the IC₅₀ concentration, the half maximal inhibitory concentration. CMOS was found to be the most potent with an IC₅₀ of 0.4148 micromolar, followed by CM18 and CDIAL with IC₅₀ concentrations of 0.9858 micromolar and 1.235 micromolar, respectively (table 2 and fig 3). Chloroquine, which was used as the positive control, had an IC₅₀ of 14.02 nanomolar, which is consistent with previously reported values.

Compounds	IC ₅₀ (μM)	Structure
CDIAL	1.235 +/- 0.135	 <p>Chemical Formula: C₁₇H₂₄O₅ Exact Mass: 308.1624</p>

CM18OX	5.016 +/- 0.372	 <p>Chemical Formula: C₃₃H₄₄O₉ Exact Mass: 584.2985</p>
CMOS	0.4148 +/- 0.038	 <p>Chemical Formula: C₁₇H₂₄O₅ Exact Mass: 308.1624</p>
UGDL	44.39 +/- 6.71	 <p>Chemical Formula: C₁₇H₂₄O₅ Exact Mass: 308.1624</p>
CM18	0.9858 +/- 0.110	 <p>Chemical Formula: C₃₄H₄₈O₁₀ Exact Mass: 616.3247</p>

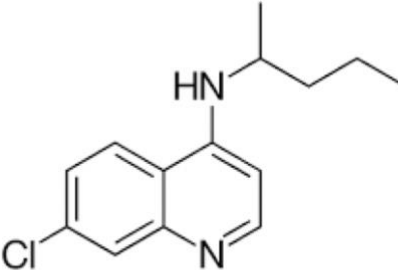
CQ	14.02 * 10 ⁻³ +/- 0.66	 <p data-bbox="878 604 1235 674">Chemical Formula: C₁₈H₂₆ClN Exact Mass: 319.9 g/mol</p>
----	-----------------------------------	--

Table 2: IC₅₀ and structures of compounds purified from *C. fragrans*. CQ, chloroquine, was used as the positive control. Data represent mean ± SD (n = 3), and one representative analysis of three bio replicates is shown.

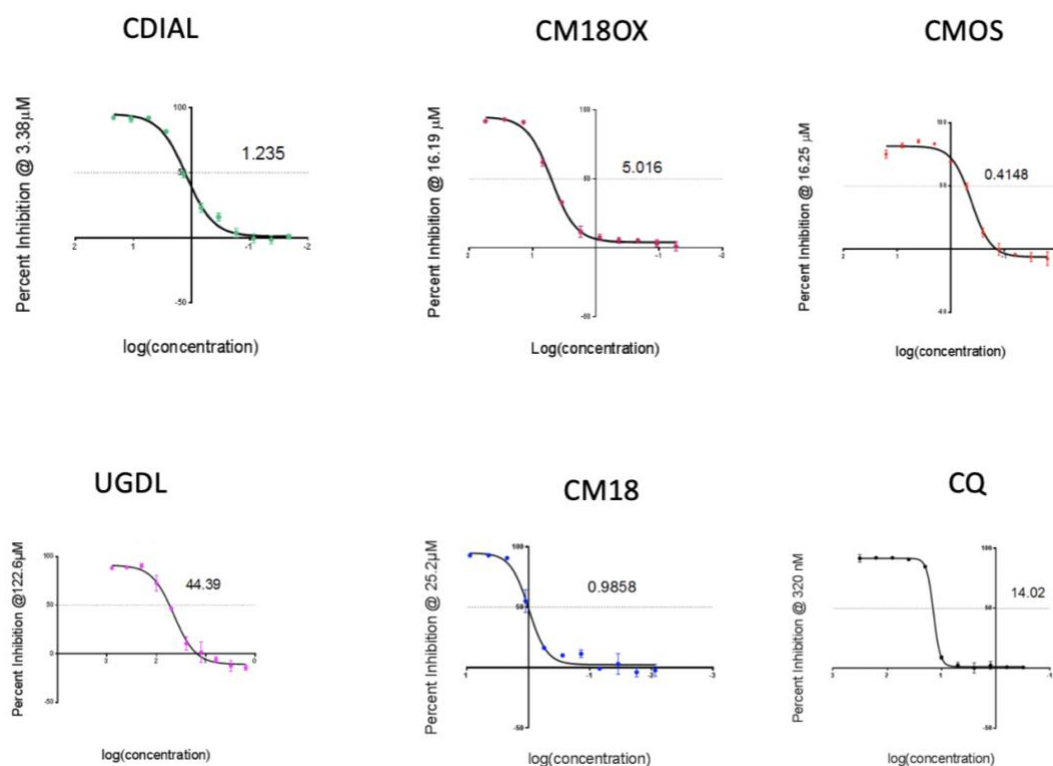


Figure 3: Non-linear regression curve fit from the 72-hour dose response assays. The percent inhibition was calculated relative to the DMSO controls. Chloroquine was used as the positive control. The IC₅₀ values are also displayed. Data represent mean ± SD (n = 3), and one representative analysis of three bio replicates is shown. Prism 8 (GraphPad) was used to create the graphs.

2.4 Discussion

The emergence and spread of *P. falciparum* resistance to Artemisinin-based treatment necessitates the search for novel therapeutics. In the past, a cell-based approach has been used in the discovery of novel therapeutics. Some of the most successful therapeutics are compounds that were purified from natural sources ([table 1](#)), artemisinin and quinine are popular examples. Thus, testing the antimalarial properties of compounds purified from natural sources is a promising field in the development of novel therapeutics.

In this study, five compounds purified from the Madagascan plant, *C. fragrans*. CDIAL, CMOS, UGDL, CM180X, and CM18 were screened for their ability to kill the asexual stages of the parasite. In order to achieve this, 72-hour drug assays were performed on a 96-well plate, and their effects were determined using flowcytometry. The percent inhibition of the drugs was calculated relative to the negative DMSO control wells, and a non-linear regression plot was used to determine the IC₅₀. CMOS had the highest potency with an IC₅₀ of 0.4148 μM, followed by CM18 with an IC₅₀ 0.958 μM. UGDL was the least potent among the compounds tested, with an IC₅₀ of 44.39 μM. Though the potency of these compounds is lower relative to the positive control, chloroquine, they are still a promising natural source for antimalarial therapeutics. This data supports previous hypothesis that *C. fragrans* has curative properties. However, these results are not indicative of - and cannot be used to infer – the effects these compounds will have in humans. There are many variables in humans that is not accounted for by this assay.

In the future, an *in vivo* model could be used, and more compounds could be purified from the bark of the plant. In addition to this, the transmission-blocking properties could be studied by determining their effect on the development and maturation of the sexual stages of *P. falciparum*

Chapter 3: Validating PfHk as a potential therapeutic target

3.1 Introduction

3.1.1 Biochemistry of the Hexokinases

PfHk is the enzyme responsible for the conversion of glucose to glucose-6-phosphate, which is consumed in glycolysis and the Pentose Phosphate Pathway (fig 4). Previous studies have shown that there is a 100-fold increase in glucose consumption in infected erythrocytes, compared to the uninfected cells (16, 17). The parasite's dependency on glycolysis as the predominant source for ATP production makes hexokinase a great target. In addition to this, even though the parasites share some identity to human hexokinase, previous studies have shown that there is a 26% identity in the amino acid sequence between PfHK and mammalian equivalent HK (18) (fig 5). This means that PfHK could be selectively inhibited without impacting mammalian hexokinase.

In mammals, the pathway that consumes the G6-P has been predicted to be affected by the expression of the different hexokinase isomers. There are four isoenzymes of Hexokinase in humans: type I, type II, type III, and type IV (glucokinase); whereas PfHk only has one isoenzyme. Type I, II, III are 100 kDa in size and glucokinase is 50 kDa (19). The four mammalian HK isozomic forms have different expression patterns which is influential in determining differences in glucose metabolism in different cells and conditions (19).

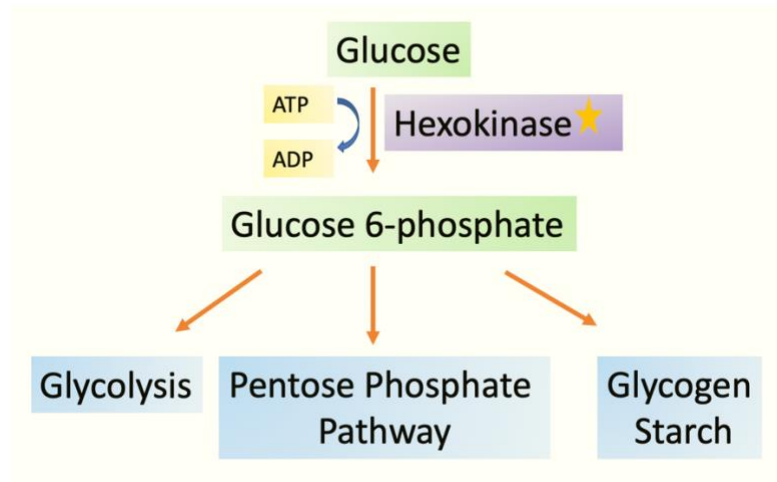


Figure 4: The fate of glucose 6-phosphate formed from the phosphorylation of glucose, via hexokinase using Mg^{2+} as cofactor (19).

3.1.2 Glucose Metabolism in *P. falciparum*

Glucose is essential for the survival of *P. falciparum*, as it is needed for ATP production, nucleic acid synthesis, and NADPH production. Metabolism of the asexual stages of the parasite is quite different from that of humans, since the parasites get most of their ATP from glycolysis and they have a dormant TCA cycle (20, 21). Specifically, *P. falciparum* uses 60-70% of the glucose supplied for glucose fermentation (22). The glucose is also used in the Pentose Phosphate Pathway (PPP) for the synthesis of ribose and NADPH. Because of the parasites rapid growth and high proliferation rates, there is a high reactive oxidative stress (ROS) in intraerythrocytic parasites (23). However, *P. falciparum* parasites have a thioredoxin system and GSH, both of which are NADPH-dependent and are used to maintain the redox equilibrium (24). Thus, the PPP plays a prominent role in the regulation of oxidative stress, since it is the only way the parasite produces NADPH.

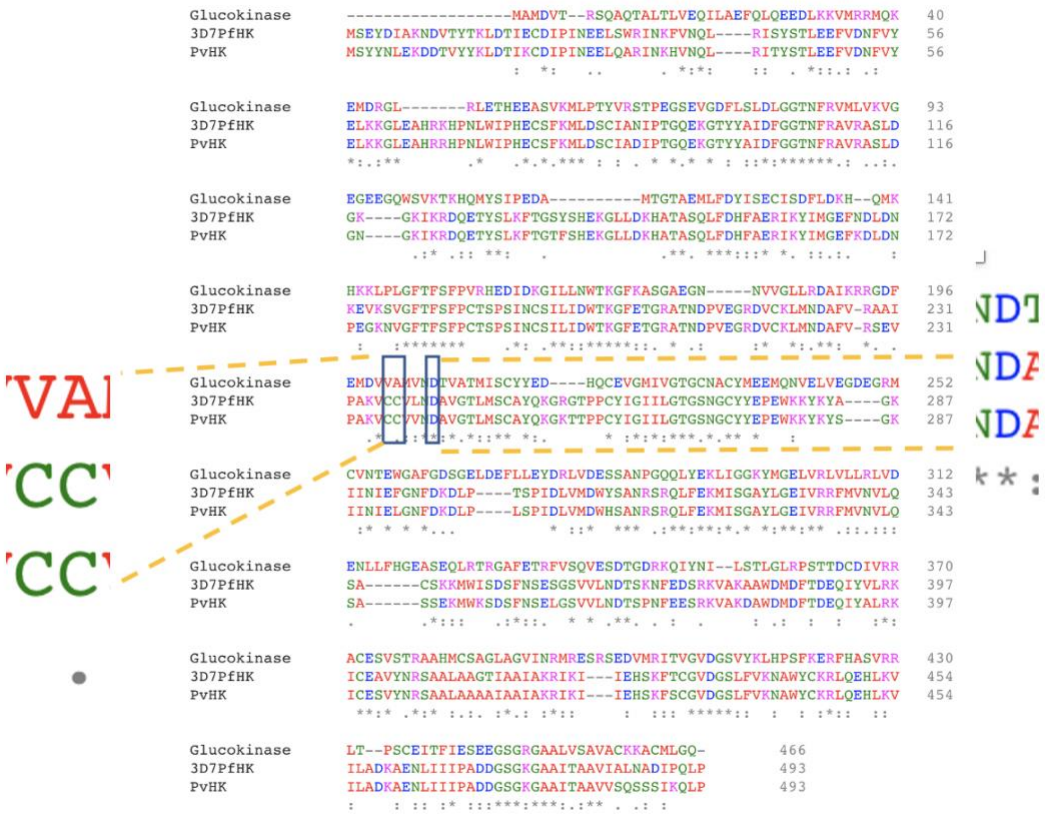


Figure 5: Alignments of MR4 3D7 PfHK, PvHK, and human glucokinase. Clustal Omega multiple sequence alignment was used. The “*” notation represents conserved amino acids. There is a 26% identity in the amino acid sequence. The amino acids highlighted are the conserved catalytic aspartate in hexokinase (Asp 241) and two cysteines that serve as a redox switch (Cys 236 and 237).

3.1.3 Life stages of the parasite and their metabolic properties

The asexual stages of the parasites rely on glycolysis for ATP production, and they have a mitochondrion with a poorly folded crista (25) that is involved in pyrimidine biosynthesis and aids the re-oxidation of membrane dehydrogenases (26). The TCA cycle is not needed for growth in the intra-erythrocytic stages of the parasite (27-29). Like the erythrocytic-asexual stages of the parasite, glycolytic enzymes are present in the sexual stages. However, they are not as

metabolically active as their asexual counterpart. There are speculations that the matured sexual stages have a more active TCA cycle, through which they get their energy (4). In addition to this, an active TCA cycle is crucial for gametocyte maturation. Other studies have shown that the mosquito stages of the parasite are more dependent on its developed TCA cycle (27-29).

Since the asexual stages of the parasite rely on glycolysis for survival and the PfHk-catalyzed reaction is hypothesized to be the rate-determining step of glycolysis, this enzyme is a promising target for future antimalarial therapeutics.

3.1.4 Post-translational modifications in PfHK

Post-translational modifications (PTM) results in the modification of pre-existing proteins in the cell, which play an important role in cell signaling, regulation, altering protein function, etc. Determining the PTMs in PfHk is of key interest as it may be used to explain the changes in glycolytic flux through the parasite cycle and how PfHk could be targeted in the synthesis of novel anti-malarial therapeutics.

Previous studies have shown that PfHK undergoes S-glutathionylation (S-Glut), a post-translational modification (**PTM**) that adds glutathione to cysteine residues (30). There are hypotheses that *S-Glut* reduces the enzyme's activity and is responsive to oxidative stress. This suggest that *S-Glut* could be important in maintaining the ATP-ADP ratio, as the parasite's demands for ATP changes.

Other PTMs are yet to be determined and their effects could provide more insights into why – and how – the activity of PfHk changes from the asexual to sexual stage.

3.2 Materials and Methods

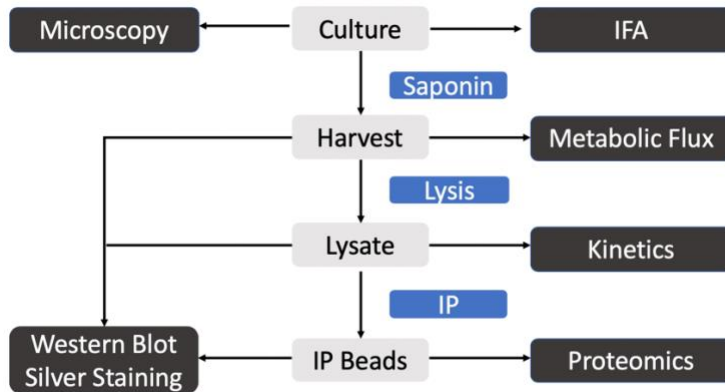


Figure 6: An overview of all the experiments conducted from MR4 3D7, cultured in O+ blood.

3.2.1 Synchronization, harvest, and lysate preparation

Synchronization

Most of the experiments conducted required a synchronized harvest for analysis. 5% D-Sorbitol was used to isolate the desired ring stage and late-stage schizont parasites. The culture was centrifuged at 3000 rpm for 5 minutes to isolate the red blood cells from the media. 10 mL of 5% D-Sorbitol was then added for every 12 mL culture, and it was incubated at room temperature for 5 minutes before centrifuging at 3000 rpm. The synchronized parasites were washed with RPMI, and it was plated with fresh RPMI + Albx with 40 μ L blood.

Parasite release

0.025% saponin was used to harvest the parasites from the red blood cells. The culture was chilled to 0°C, and it was centrifuged at 3000 rpm for 5 minutes. For every 12 mL culture that was centrifuged, 10 mL of 0.025% saponin was added, incubated for 5 minutes till RBC lysis

was evident, and it was centrifuged at 3000 rpm to isolate the parasites. The parasites were then washed with PBS and were stored at -80°C in PBS containing protease inhibitors.

Lysate Preparation

Harvested parasites that were stored at -80°C were lysed, via a series of freeze-thaw cycles. For each lysis, the parasites went through three freeze-thaw cycles, before they were centrifuged at 20,817 RCF at 4°C for 20 minutes to isolate the fractionate the insoluble cell content from the soluble content. The supernatant, containing the PfHK protein was isolated, and it was used for all experiments.

3.2.2 PfHK antiserum production and purification

Rabbit polyclonal antibodies were raised using recombinant PvHK (ref) kindly supplied by the Morris Lab, Clemson University, SC. All procedures of raising antibody and collecting rabbit antisera was done by Thermo Scientific. The polyclonal antibodies were affinity purified using AminoLink antibody purification kit (Thermo Scientific), and its efficacy was tested using recombinant *P. vivax* hexokinase and parasite lysates.

3.2.3 Recombinant Pv-HK Generation

Plasmodium vivax hexokinase (Uniprot ID: A5K274) was generated by expressing it in *Escherichia coli* BL21. A codon-optimized open reading frame cloned into a pQE30 expression vector (Qiagen, Valencia, CA) was used. The protein was purified as described by Davis et. al.

3.2.4 SeaHorse XF glycolytic rate assay

The Agilent SeaHorse XF measures glycolytic rate by measuring real-time proton efflux, the extracellular acidification rate (ECAR). The instructions on the XF kit was used, in combination with the protocol described by Sakata-Kato et. al. (31). The cartridge was hydrated overnight at 37°C in XF Calibrant solution. The injections were loaded onto the cartridge after doing a media change. On the day of the assay, the infected RBC were isolated from uninfected RBC using a MACS separation column by Miltenyi Biotec. The number of cells were counted, and it was adjusted accordingly for the assays. In most cases 10 – 12 million parasites/ 100 µL were used. The synchronized parasites were then harvested, centrifuged, and resuspended in the assay medium. 100 µL of the parasites were loaded to each well and it was centrifuged at 52 rcf for 5 minutes, followed by the addition of 350 µL of the assay medium (31). Following the plating procedure, the temperature was increased to 37°C before determining the ECAR.

3.2.5 Kinetic Assays

The “Kinetic Assay NADPH path check” protocol on the SoftMax Pro software was used for all kinetic assay that was performed in this experiment. All kinetic experiments were performed on the SpectraMax i3x at 340 nm, 37°C for 30 minutes at 45 seconds interval. The assay was set-up in a clear bottom 96-well plate. The total reaction volume was 100 µL. 78 µL of the “master mix” was added, followed by 20 µL of lysate or PvHK in PBS plus protease inhibitors, and then 2 µL of 1M glucose. The master mix was made up of TAE buffer (pH 7.4), MgCl₂, NADP, Glucose-6-phosphate dehydrogenase, and ATP. The final reaction contained 50 mM TAE buffer, 3.3 mM MgCl₂, 0.75 mM NADP, Glucose-6-phosphate dehydrogenase, and 5.25 mM ATP.

Mechanism of Kinetic Assay

The activity of PfHK was determined by measuring the absorbance of NADP⁺ at 340 nm. The absorbance value was then used to determine the amount of G-6-P produced by hexokinase, which is a measurement of the enzyme's activity (fig 6). The SoftMax Pro software was programmed to perform these calculations, so it converted the raw data files to the velocity of PfHK at different timepoints.

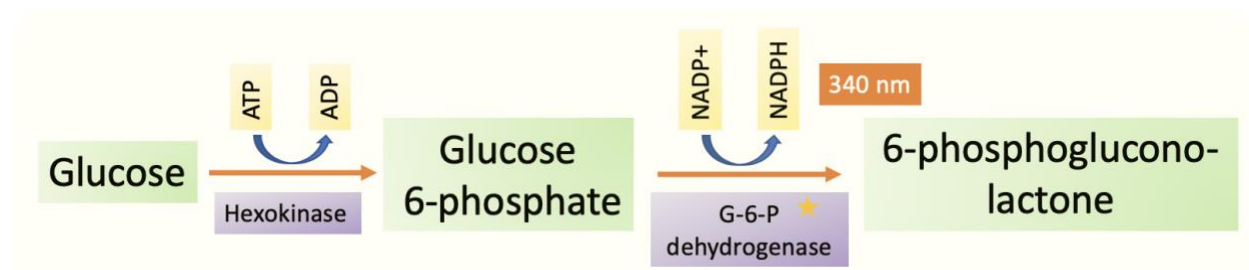


Figure 7: NADP⁺ coupled enzymatic assay. The activity of PfHK was determined by measuring the absorbance of NADP⁺ at 340 nm.

ATP and glucose kinetic assays

For the ATP-dependent and glucose-dependent kinetic reactions, the maximum concentration of ATP and glucose were set at 20 mM and the a five-fold dilution was performed. The same amount of parasite was used for both reactions.

Time-point kinetic assays

Synchronized *P. falciparum* 3D7 parasites were expanded to 14 plates and were allowed to grow to approximately 7% parasitemia. On day 0, all cultures were synchronized and six, 30 mL cultures were produced. A plate was harvested at 0, 13, 24, 30, 37, and 42 hours, with each time point corresponding to a specific asexual life stage (fig 2). These samples were stored at -80°C

and were used to determine how the activity of HK changes through the life stages of the parasite. Fresh whole cell lysates were prepared on the day of the assay, and same volume of lysate was added to each well. The recombinant PvHk was used as the positive control. The remainder of the samples were analyzed on an SDS-PAGE gel to confirm the presence of PfHk and to estimate its concentration.

3.2.6 Western Blots

SDS-PAGE gels

All samples were added to 4x loading dye to produce a 1x solution. The 1x solution was heated at 95°C for 5 minutes, before the samples were loaded on a Mini-PROTEAN® TGX Stain-Free™ Precast Gels. Precision Plus Protein™ Dual Color Standards marker was used, and the gel was run at 180 V for approximately an hour in 1x running SDS-buffer. The gel was equilibrated for 10 minutes in wet-transfer buffer, before transferring the protein to a PVDF membrane at 100 volts for 30 – 45 minutes. The membrane was blocked in 5% TBST-milk (non-fat) for 30 minutes at room temperature, before incubating in primary overnight (1:500) at 4°C. The membrane was then incubated in secondary Goat-antirabbit (GAR, 1:2000), and the western blot signal was detected using SuperSignal West Pico PLUS chemiluminescent substrate kit (Thermo Scientific).

Non-reducing conditions

Regular conditions were used for non-reducing conditions with a few changes. The 4x loading buffer used did not contain any 2-mercaptoethanol. The running buffer and wet-transfer buffer used for reducing conditions were used in non-reducing as well.

Native conditions

Regular conditions were used for native conditions with a few changes. The running buffer and wet-transfer buffer that were used did not contain any SDS. In addition to this, 4x native loading buffer used and the samples were heated for a minute at 95°C.

3.2.7 Estimating protein concentration

BCA assay

The Thermo Scientific™ Pierce™ BCA Protein Assay Kit was used to determine for the quantification and coulometric detection of protein present in the samples. The BSA albumin standards were prepared using the protocol in the user guide. The BCA working reagent was created by mixing 50 parts of BCA reagent A and 1 part of BCA reagent B. 25 µL of the unknown and standard were plated on a 96-well clear microplate, followed by 200 µL of the working reagent. The plate was incubated at 37°C for 30 minutes, after which the absorbances were recorded at 562nm on the SpectraMax i3x.

Determining concentration of PfHk in stage-specific harvests

The protein concentration of PfHK was estimated using Image J. The concentration of recombinant Pv-HK was determined using BCA assay. A two-field serial dilution of PvHk and the stage-specific PfHk harvest was run under reducing conditions. The western blots were scanned using an Epson V600 scanner. A professional, 16-bit gray scale, 4600 dpi image was produced which was saved as a .tiff raw file. The “rectangle” feature on ImageJ was used to create a frame of known area, and this frame was used to measure the intensities of the region of interests. The intensities of the region below and above each band were determined, which served as the background for the calculations. The PvHk intensity values were used to create a standard graph, which was used to estimate the concentration of PfHK.

3.2.8 Immunoprecipitation and proteomic analysis

Immunoprecipitation

Cultured MR4 3D7 were harvested using 0.025% saponin, followed by a series of freeze-thaw cycles to lyse the parasites. The Pierce Crosslink Immunoprecipitation Kit was used for the immunoprecipitation of PfHK and the standard instructions were used. The lysate was pre-cleared using coupling buffer. 50 µL of the slurry protein A/G and 50 µL of the HK primary antibody were incubated on a rocking platform for an hour to allow the antibody to bind to the beads. The beads were then washed, and the lysate was added to it. This was followed by an overnight incubation at 4°C. The beads were then washed with lysis buffer, followed by an elution buffer. Successful completion of immunoprecipitation was confirmed by silver staining and western blotting.

Proteomic Analysis

The immunopurified PfHK beads were analyzed via silver staining and Coomassie blue staining to confirm presence of the protein. The beads were then submitted to proteomics to search for any modifications and to determine the exact mass of the protein.

3.2.9 Immunofluorescence assay

Blood smears were made from asynchronous parasites, followed by immersing the slides in an Acetone-Methanol mix (50:50) and incubating in -20°C for 10 minutes. The smears were washed with 1X PBS, blocked in 1% BSA in 1X PBT for one hour, and were incubated overnight with rabbit anti- PfHK antibody at 4°C. Slides were washed with 1X PBS to remove unbound antibody and incubated with fluorescence tagged Goat anti-rabbit secondary antibody

(Life Technologies) for one hour at room temperature. Afterwards, slides were once again washed with 1X PBS and covered with a coverslip using Prolong Diamond Antifade 1 (Life Technologies) with DAPI mounting medium. The slides were scanned using the FV300 Olympus Confocal Laser Scanning Microscope at a 60X magnification. Invitrogen Alexa Fluor® 488, with an excitation at 488 nm, and Thermo Scientific Pierce DAPI Nuclear Counterstains were used.

3.3 Results

3.3.1 Matured sexual stages are glycolytically inactive

Following the isolation of purified parasites, the SeaHorse XF analyzer was used to determine the glycolytic flux on MR4 3D7 parasites. The starting extracellular acidification rate (ECAR) of a million parasite for the asexual stages was 100 mpH/min, compared to 5 mpH/min for the matured sexual stages (fig 8). As expected, the uninfected red blood cell had an insignificant change in ECAR. At 20 minutes, 500 μ M of 2-deoxyglucose (2DG) was added which resulted in a sharp decrease in ECAR for the asexual stages of the MR4. However, the sexual stages did not experience a notable change in the ECAR post-injection. In both the asexual and sexual stages, there was a decline in the ECAR overtime.

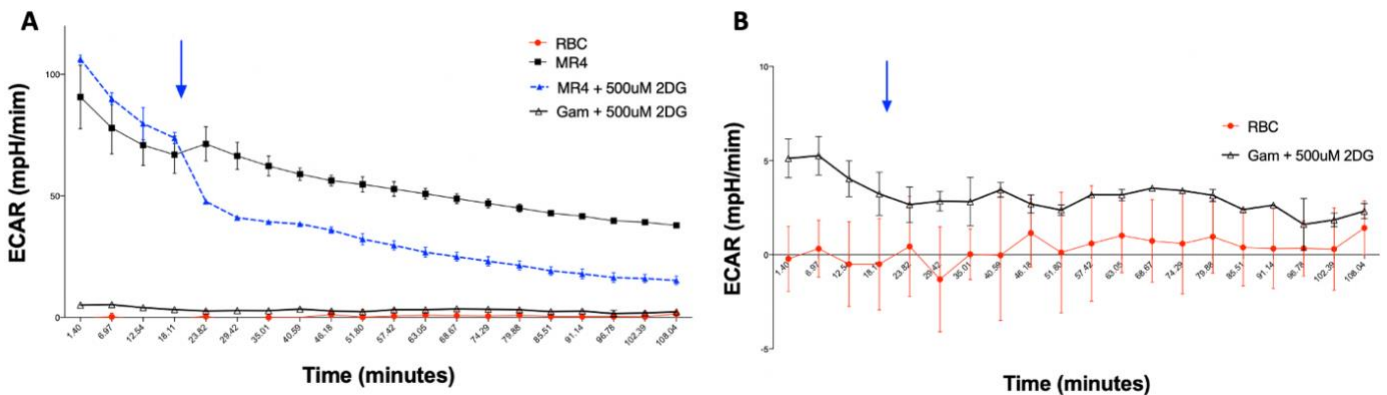


Figure 8: Extracellular acidification rate (ECAR) of synchronized asexual schizont stages MR4 3D7 and matured gametocytes were measured on the SeaHorse XF Analyzer. Approximately, one million cells were present in each well. The ECAR was measured before and after the addition of 500 μ M of 2-deoxyglucose at 20 minutes. **B** shows the activity of the sexual stages and the red blood cells.

3.3.2 Expression and cellular localization of PfHK

IFAs were performed to determine the expression of PfHK in the different stages of *P. falciparum* and to determine the cellular localization of PfHK in the cell. In the field chosen for the asexual stages, there is an invading merozoite, a ring, trophozoite, and a schizont. For the matured gametocytes, there is a matured male and female gametocyte present in the selected field. PfHk was expressed in the cytosol in all the human life-stages of the parasite ([fig 9](#) and [fig 10](#)).

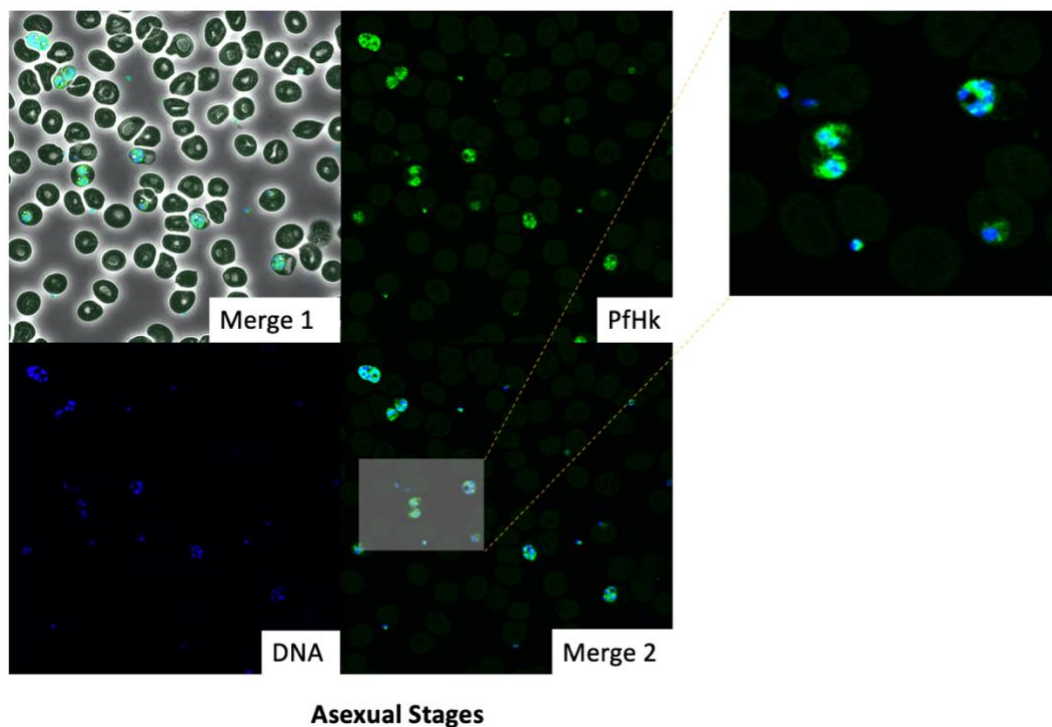


Figure 9: IFA assays for the asexual MR4 3D7 parasites. 8a (merge 1): Composite image of PfHk, DNA, and light microscopy. 8b (DNA): Nuclei were stained with DAPI. 8c (PfHk): PfHk stained green with Alexa Fluor® 488. 8d

(merge 2): Composite image of DNA and PfHk. The enlarged image shows a merozoite preparing to invade a red blood cell to form a ring.

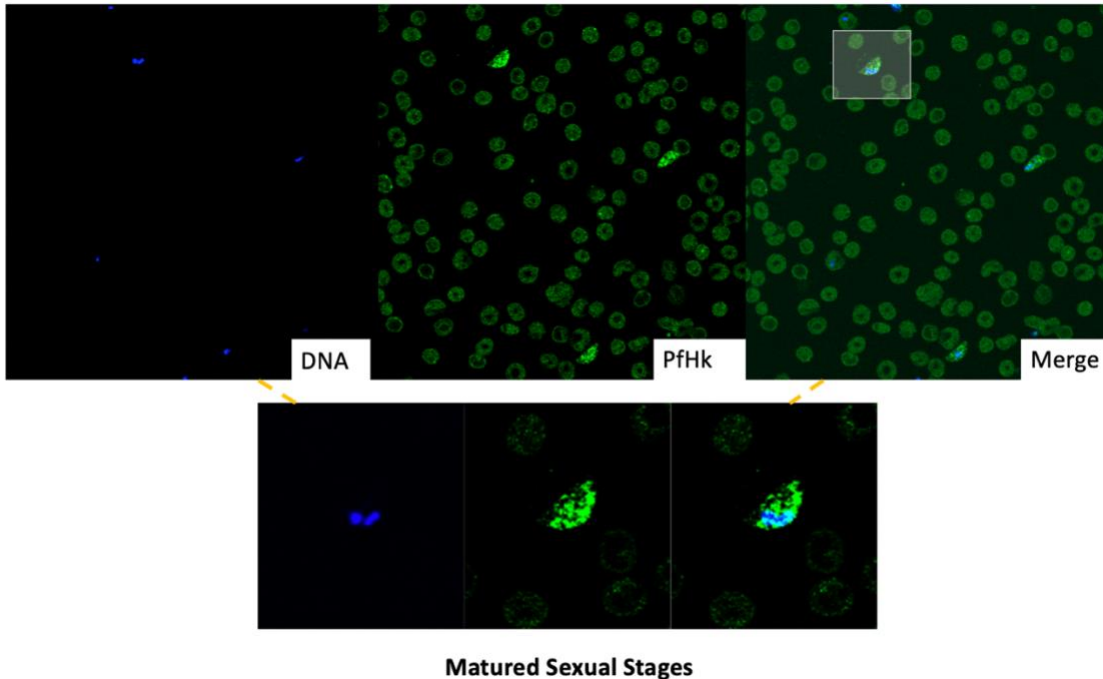


Figure 10: IFA assays for the matured sexual MR4 3D7 parasites. 9a (DNA): Nuclei were stained with DAPI. 9b (PfHk): PfHk stained green with Alexa Fluor® 488. 9c (merge): Composite image of DNA and PfHk. The smaller panels are an enlarged view of a matured gametocyte.

3.3.3 Biochemical properties of PfHk and copies of PfHk in a parasite

The BCA assay was used to determine the total protein concentration in the rings, trophozoites, and schizonts stages. The schizonts had the highest total protein content, followed by the trophozoites, then the ring stages. The trophozoites had the highest percentage (2.30%) of hexokinase per total protein in the parasite; whereas the rings and schizonts were comparable (0.2%) (table 3). In addition to this, the number of PfHK molecules in a parasite was estimated using the total parasite and the estimated protein concentration from the PvHk pixel intensity

analysis. The trophozoites had the highest HK molecules per parasite, with an estimated value of 6.8×10^6 , followed by schizonts at 7.7×10^5 , and the rings stages at 2.8×10^5 (table 3).

The kinetic parameters of PfHK were determined using the glucose 6-phosphate dehydrogenase coupled assay. The absorbances were used to determine the maximum rate of reaction (V_{max}), Michaelis constant (K_m), and the catalytic efficiency (k_{cat}), using varying concentrations of glucose and ATP in the rings, trophozoites, schizonts, and matured gametocyte stages. Sufficient activity was not detected for the sexual stages, so these values were not reported. A substrate curve and a double-reciprocal plot were used to represent data (fig 12). PfHk's affinity for glucose and ATP were similar for the rings, trophozoites, and schizonts, with the trophozoites showing the highest affinity for glucose (0.095 mM) and the rings showing the highest affinity for ATP (0.186 mM). The trophozoites had the lowest turnover rate, K_{cat} , for both ATP and glucose; whereas the rings and schizonts had a higher K_{cat} (table 3).

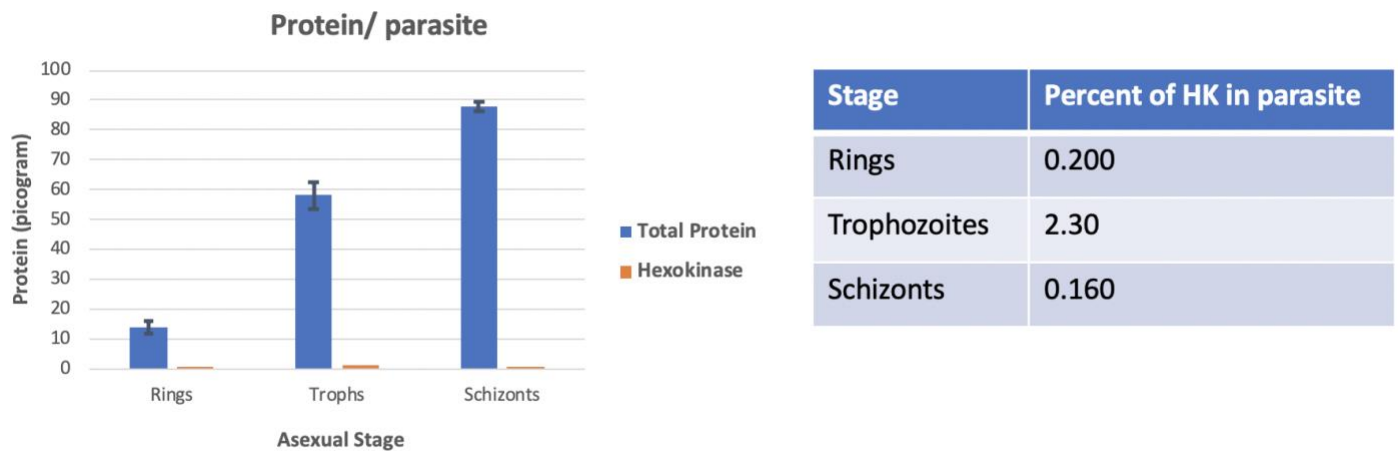


Figure 11: Protein content for rings, trophozoites, schizonts. The total protein amount in a parasite was determined using the BCA assay. The estimated amount of PfHk was determined a series of western blot analysis. Data represent mean \pm SD (n = 3).

Table 3: The percentage of PfHk relative to the total mass of protein in the different stages of the parasite. Data represent mean \pm SD (n = 3).

	Glucose		ATP		
	K_m (mM)	k_{cat} (min ⁻¹)	K_m (mM)	k_{cat} (min ⁻¹)	HK molecules per parasite
Rings	0.131	18.3×10^6	0.186	17.5×10^6	2.78×10^5
Trophozoites	0.0954	4.63×10^6	0.257	5.07×10^6	6.83×10^6
Schizonts	0.136	23.6×10^6	0.250	25.8×10^6	7.70×10^5
Gametocytes	No activity detected				

Table 4: K_m and K_{cat} of PfHK during its different life stages. The number of HK molecules per parasite are also shown, estimated using the amount of PfHK in the lysates.

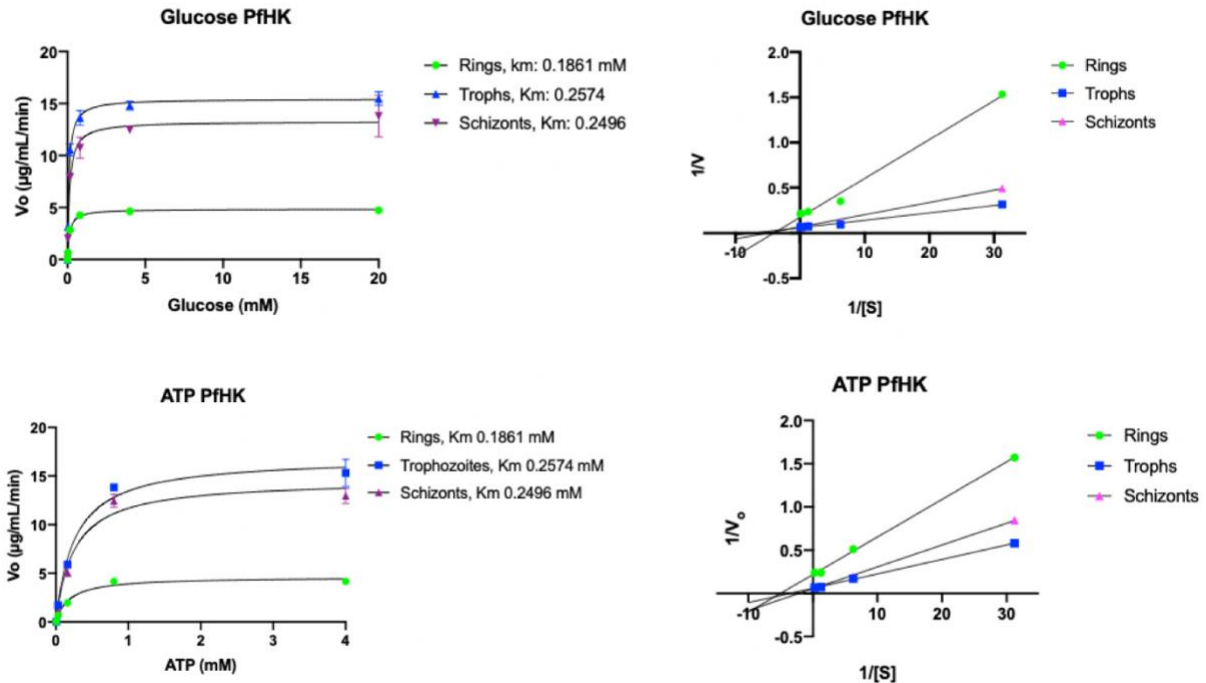


Figure 12: The substrate curve and double-reciprocal (Lineweaver-Burk) plots for the stage-specific harvest kinetic assays for glucose and ATP. Data represent mean \pm SD ($n = 3$). One of two bio-replicates is shown.

Time point kinetic assay

Synchronized asexual *P. falciparum* were harvested at different time points, and their lysates were used to determine the activity of PfHk through the intra-erythrocytic life cycle of the parasite. Five different time points, corresponding to the major development stages in the asexual parasite were used (fig 2). Equal volume of lysates was used for each time point, and the absorbances were measured using NADP⁺-coupled enzymatic assay. During the first half of the life cycle, the V_{\max} observed increased till it reached its peak 24 hours post-invasion, which corresponds to the trophozoite stages (fig 13). After the 24 hours, there is a rapid decline of the V_{\max} at a similar rate to the first 24 hours.

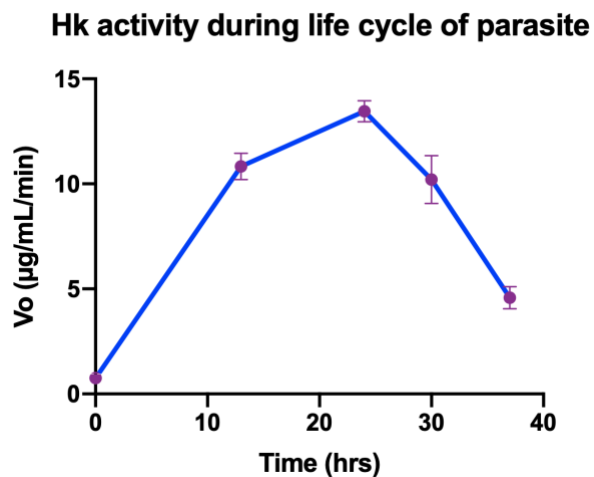


Figure 13: The activity of PfHk in the asexual stages, during its 44-hour life cycle, measured using the *in vitro* kinetic assays. The V_{\max} at different time-points post-invasion are shown. Data represent mean \pm SD ($n = 3$). One of two bio replicates is shown.

3.3.4 PfHK is a tetramer *in vivo*

PfHK and recombinant PvHK were analyzed using western blots in both reducing and native conditions. In native conditions, PfHK 3D7 was a tetramer at ~220kD; whereas in reducing conditions, it was a monomer at ~55kD (Fig. 14). PfHk was expressed in the sexual stages, and the expressed protein similar results to those in the asexual stages.

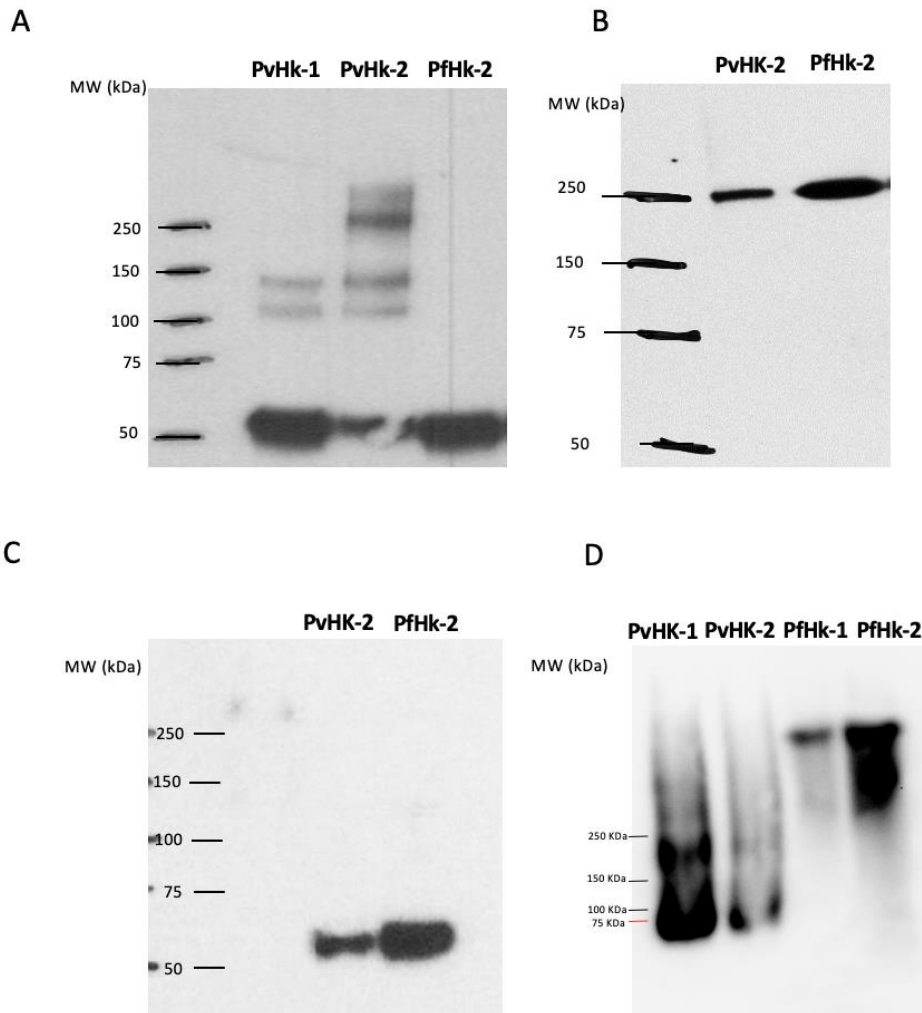


Figure 14: Western blots of native PfHK and recombinant Pv-HK. (A) SDS-PAGE of asynchronized asexual stages. (B) NATIVE-PAGE of asynchronized asexual stages. (C) SDS-PAGE of matured sexual stages. (D) NATIVE-PAGE of matured sexual stages. Two dilutions of PvHK were used in (a) and (d), which are depicted as PvHk-1 and PvHk-2. Two dilutions of PfHk were used in (d), depicted as PfHk-1 and PfHk-2.

3.3.5 Immunoprecipitation

PfHk was immunopurified for proteomic analysis using the Pierce™ Classic IP Kit. Western blot and silver staining were used to confirm successful isolation of the protein and to determine the relative amount present in the elution and mock, respectively. The mock IP served as a negative control in the experiment to ensure that the protein bands on the western were due to the expression of PfHk and not protein A/G. PfHk was successfully isolated in elution 1 (fig 15). The samples were sent to proteomics, where the post-translational modifications would be determined and analyzed.

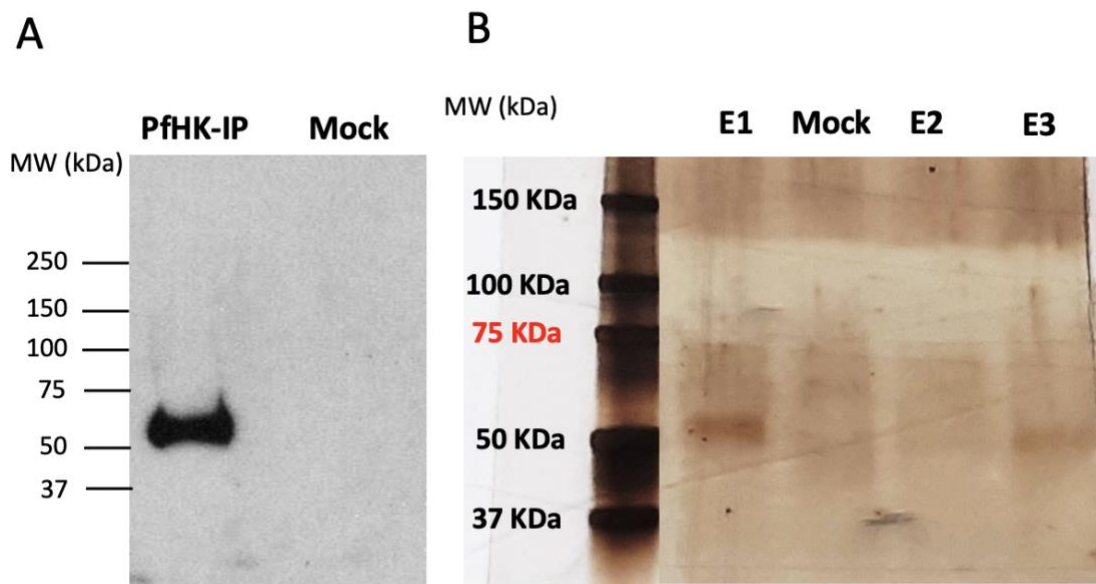


Figure 15: Immunoprecipitations of PfHK. (A) SDS PAGE of immunopurified PfHK (E1) and mock IP beads. (B) Silver staining of immunopurified PfHK (E1, E2, E3) and mock IP beads. PfHk-IP is the immunopurified protein and the mock IP is protein A/G beads. E represents the elution and the number signifies the order of elution, such that E1 is the first elution.

3.4 Discussion

The intraerythrocytic life stages of *P. falciparum* relies on the activity of PfHk for survival since it produces glucose 6-phosphate, a substrate for ATP generation in glycolysis and oxidative stress regulation in the pentose phosphate pathway (PPP). Previous studies have shown that inhibition of glycolysis, via small-molecule compounds that block hexose transport, results in potent antimalarial activity (32). Thus, PfHk could serve as a potential target in the parasite.

In this study, PfHk was characterized through different approaches. A polyclonal PfHk antibody was generated which was used to determine the biochemical properties, expression, and localization of the enzyme. In addition to this, a series of assays were performed to determine the glycolytic flux of the asexual and sexual stages of the parasite. The characterization of PfHk revealed that it shares similar properties with mammalian hexokinase, including the cytosolic expression of the enzyme in both the asexual and sexual stages a (fig 9 and 10). Taking advantage of the generated poly-clonal antibody, western blots analysis was used to support previous hypothesis that the enzyme is a tetramer *in vivo*. Western blotting of *P. falciparum* whole-cell lysate under reducing and native conditions recognized bands at ~55kDa and ~220 kDa (fig 14), which are suggestive that the enzyme is a homotetramer *in vivo*. These results are also supported by recently published structural studies of recombinant PvHk by a collaborating lab (1).

Data from the SeaHorse XF assays show that the asexual stages of the parasites exhibit a lot of glycolytic activity and are inhibited by 2-deoxyglucose, a competitive inhibitor of Hk. For the sexual stages, on the other hand, similar amount of parasite resulted in a twenty-fold reduction in glycolytic activity. These results support previous hypothesis that the sexual stages are glycolytically dormant (4). Interestingly, images from the IFAs show that PfHK is expressed

in both the sexual and asexual stages of the parasite. Even though this assay does not provide information on the integrity or form of the parasite, it is reasonable to hypothesize that Hk is undergoing modifications that decrease its activity as the parasite develops into a matured sexual stage and switches to a more active TCA cycle. Thus, if PfHk is indeed the rate-limiting step of glycolysis then it could have an influential role in the initiation and development of gametocytes.

In order to learn more about how the amount and activity of PfHK changes through the life cycle of the parasite, *in vitro* kinetic assays were performed with lysates of the asexual and sexual stages. These assays showed that the enzyme's affinity for glucose and ATP were similar across the different stages, however their catalytic efficiencies were different. Specifically, the trophozoites had the lowest catalytic efficiency, followed by the rings, and then the schizonts. These results are interesting since the trophozoites would be expected to have the highest turnover rate due to their high metabolic activity. However, the loss in efficiency is made up for by the number of Hk molecules in a parasite. A trophozoite has approximately 7 million copies of Hk, which is 25 times the Hk molecules in a ring and 10 times the HK molecules in a schizont ([table 4](#)). In addition to this, results from the BCA assay show that the trophozoites have a higher ratio of Hk to total protein in the parasite. The huge amount of Hk copies and protein mass compensate for the needs of a growing trophozoite. The loss in catalytic efficiency from a ring to a trophozoite might be due to modifications associated with increased oxidative stress in the parasite. Therefore, determining possible modifications could be helpful in understanding the enzyme's regulation.

There are several observations that validate why PfHk could serve as a potential antimalarial target. First, the enzyme is needed for glycolysis and PPP, because it catalyzes the first step in both processes. Thus, without this enzyme, sufficient ATP cannot be generated in the

asexual stages of the parasite and there would be no regulation of oxidative stress. Second, PfHk shares only 26% (fig 5) of its identity with the mammalian hexokinase, which makes it possible for PfHk to be specifically targeted (33). The third reason is that the SeaHorse XF assays data (fig 8) showed that when a glucose substrate analog, 2-deoxyglucose, was used the glycolytic rate decreased almost immediately, which is suggestive of the idea that there are no alternative pathways for the parasite without the action of PfHk. Finally, the results from the immunofluorescence assays (fig 9) and western blots (fig 14) showed that PfHk is expressed in the sexual stages, however there no PfHk activity was detected in the kinetic assays (table 4). This means that PfHk undergoes changes during gametocytogenesis that decreases its activity. Though the reasons for this are yet to be determined, unravelling the mechanisms/ processes that occur could provide more knowledge on how PfHk could be targeted.

Future directions include identifying post-translational modifications in the specific stages of the parasite and determining the role they play in PfHk expression and activity.

References

1. Srivastava SS, Darling JE, Suryadi J, Morris JC, Drew ME, Subramaniam S. Plasmodium vivax and human hexokinases share similar active sites but display distinct quaternary architectures. *IUCrJ*. 2020;7(3). doi: doi:10.1107/S2052252520002456.
2. WHO. World Malaria Report 2019 2019 [cited 2020 January]. Available from: https://www.who.int/malaria/publications/world_malaria_report/en/.
3. Sinden RE. Sexual development of malarial parasites. *Adv Parasitol*. 1983;22:153-216. Epub 1983/01/01. doi: 10.1016/s0065-308x(08)60462-5. PubMed PMID: 6141715.
4. Talman AM, Domarle O, McKenzie FE, Arie F, Robert V. Gametocytogenesis: the puberty of Plasmodium falciparum. *Malar J*. 2004;3:24. Epub 2004/07/16. doi: 10.1186/1475-2875-3-24. PubMed PMID: 15253774; PMCID: PMC497046.
5. Bruce MC, Alano P, Duthie S, Carter R. Commitment of the malaria parasite Plasmodium falciparum to sexual and asexual development. *Parasitology*. 1990;100 Pt 2:191-200. Epub 1990/04/01. doi: 10.1017/s0031182000061199. PubMed PMID: 2189114.
6. Silvestrini F, Alano P, Williams JL. Commitment to the production of male and female gametocytes in the human malaria parasite Plasmodium falciparum. *Parasitology*. 2000;121 Pt 5:465-71. Epub 2000/12/29. doi: 10.1017/s0031182099006691. PubMed PMID: 11128797.
7. Yeung S. Malaria-Update on Antimalarial Resistance and Treatment Approaches. *Pediatr Infect Dis J*. 2018;37(4):367-9. Epub 2018/01/10. doi: 10.1097/INF.0000000000001887. PubMed PMID: 29315159.
8. CDC. illustration of the life cycle of the parasites of the genus, Plasmodium, that are causal agents of malaria: CDC; 2002 [cited 2020 January].
9. Molnar P, Marton L, Izrael R, Palinkas HL, Vertessy BG. Uracil moieties in Plasmodium falciparum genomic DNA. *FEBS Open Bio*. 2018;8(11):1763-72. Epub 2018/11/10. doi: 10.1002/2211-5463.12458. PubMed PMID: 30410856; PMCID: PMC6212640.
10. Inocente EA, Nguyen B, Manwill PK, Benatrehina A, Kweka E, Wu S, Cheng X, Rakotondraibe LH, Piermarini PM. Insecticidal and Antifeedant Activities of Malagasy Medicinal Plant (Cinnamosma sp.) Extracts and Drimane-Type Sesquiterpenes against Aedes aegypti Mosquitoes. *Insects*. 2019;10(11). Epub 2019/11/17. doi: 10.3390/insects10110373. PubMed PMID: 31731570; PMCID: PMC6920793.
11. Randrianarivelosia M, Rasidimanana VT, Rabarison H, Cheplogoi PK, Ratsimbason M, Mulholland DA, Mauclere P. Plants traditionally prescribed to treat tazo (malaria) in the eastern region of Madagascar. *Malar J*. 2003;2:25. Epub 2003/08/19. doi: 10.1186/1475-2875-2-25. PubMed PMID: 12921540; PMCID: PMC184444.
12. Tse EG, Korsik M, Todd MH. The past, present and future of anti-malarial medicines. *Malar J*. 2019;18(1):93. Epub 2019/03/25. doi: 10.1186/s12936-019-2724-z. PubMed PMID: 30902052; PMCID: PMC6431062.
13. WHO. The WHO Model List of Essential Medicines. 2019.
14. Davis MI, Patrick SL, Blanding WM, Dwivedi V, Suryadi J, Golden JE, Coussens NP, Lee OW, Shen M, Boxer MB, Hall MD, Sharlow ER, Drew ME, Morris JC. Identification of Novel Plasmodium falciparum Hexokinase Inhibitors with Antiparasitic Activity. *Antimicrob Agents Chemother*. 2016;60(10):6023-33. Epub 2016/07/28. doi: 10.1128/AAC.00914-16. PubMed PMID: 27458230; PMCID: PMC5038330.
15. Fivelman QL, McRobert L, Sharp S, Taylor CJ, Saeed M, Swales CA, Sutherland CJ, Baker DA. Improved synchronous production of Plasmodium falciparum gametocytes in vitro.

- Mol Biochem Parasitol. 2007;154(1):119-23. Epub 2007/05/25. doi: 10.1016/j.molbiopara.2007.04.008. PubMed PMID: 17521751.
16. Pfaller MA, Krogstad DJ, Parquette AR, Nguyen-Dinh P. Plasmodium falciparum: stage-specific lactate production in synchronized cultures. Exp Parasitol. 1982;54(3):391-6. Epub 1982/12/01. doi: 10.1016/0014-4894(82)90048-0. PubMed PMID: 6759150.
 17. Roth EF, Jr., Raventos-Suarez C, Perkins M, Nagel RL. Glutathione stability and oxidative stress in P. falciparum infection in vitro: responses of normal and G6PD deficient cells. Biochem Biophys Res Commun. 1982;109(2):355-62. Epub 1982/11/30. doi: 10.1016/0006-291x(82)91728-4. PubMed PMID: 6758788.
 18. Olafsson P, Matile H, Certa U. Molecular analysis of Plasmodium falciparum hexokinase. Mol Biochem Parasitol. 1992;56(1):89-101. Epub 1992/11/01. doi: 10.1016/0166-6851(92)90157-f. PubMed PMID: 1475005.
 19. Wilson JE. Isozymes of mammalian hexokinase: structure, subcellular localization and metabolic function. J Exp Biol. 2003;206(Pt 12):2049-57. Epub 2003/05/21. doi: 10.1242/jeb.00241. PubMed PMID: 12756287.
 20. Kirk K, Horner HA, Kirk J. Glucose uptake in Plasmodium falciparum-infected erythrocytes is an equilibrative not an active process. Mol Biochem Parasitol. 1996;82(2):195-205. Epub 1996/11/25. doi: 10.1016/0166-6851(96)02734-x. PubMed PMID: 8946385.
 21. van Dooren GG, Stimmler LM, McFadden GI. Metabolic maps and functions of the Plasmodium mitochondrion. FEMS Microbiol Rev. 2006;30(4):596-630. Epub 2006/06/16. doi: 10.1111/j.1574-6976.2006.00027.x. PubMed PMID: 16774588.
 22. Jensen MD, Conley M, Helstowski LD. Culture of Plasmodium falciparum: the role of pH, glucose, and lactate. J Parasitol. 1983;69(6):1060-7. Epub 1983/12/01. PubMed PMID: 6371212.
 23. Becker K, Tilley L, Vennerstrom JL, Roberts D, Rogerson S, Ginsburg H. Oxidative stress in malaria parasite-infected erythrocytes: host-parasite interactions. Int J Parasitol. 2004;34(2):163-89. Epub 2004/03/24. doi: 10.1016/j.ijpara.2003.09.011. PubMed PMID: 15037104.
 24. Preuss J, Jortzik E, Becker K. Glucose-6-phosphate metabolism in Plasmodium falciparum. IUBMB Life. 2012;64(7):603-11. Epub 2012/05/29. doi: 10.1002/iub.1047. PubMed PMID: 22639416.
 25. Das A, Syin C, Fujioka H, Zheng H, Goldman N, Aikawa M, Kumar N. Molecular characterization and ultrastructural localization of Plasmodium falciparum Hsp 60. Mol Biochem Parasitol. 1997;88(1-2):95-104. Epub 1997/09/01. doi: 10.1016/s0166-6851(97)00081-9. PubMed PMID: 9274871.
 26. Krungkrai J. Purification, characterization and localization of mitochondrial dihydroorotate dehydrogenase in Plasmodium falciparum, human malaria parasite. Biochim Biophys Acta. 1995;1243(3):351-60. Epub 1995/04/13. doi: 10.1016/0304-4165(94)00158-t. PubMed PMID: 7727509.
 27. MacRae JI, Dixon MW, Dearnley MK, Chua HH, Chambers JM, Kenny S, Bottova I, Tilley L, McConville MJ. Mitochondrial metabolism of sexual and asexual blood stages of the malaria parasite Plasmodium falciparum. BMC Biol. 2013;11:67. Epub 2013/06/15. doi: 10.1186/1741-7007-11-67. PubMed PMID: 23763941; PMCID: PMC3704724.
 28. Ke H, Lewis IA, Morrissey JM, McLean KJ, Ganesan SM, Painter HJ, Mather MW, Jacobs-Lorena M, Llinas M, Vaidya AB. Genetic investigation of tricarboxylic acid metabolism

- during the *Plasmodium falciparum* life cycle. *Cell Rep.* 2015;11(1):164-74. Epub 2015/04/07. doi: 10.1016/j.celrep.2015.03.011. PubMed PMID: 25843709; PMCID: PMC4394047.
29. Sturm A, Mollard V, Cozijnsen A, Goodman CD, McFadden GI. Mitochondrial ATP synthase is dispensable in blood-stage *Plasmodium berghei* rodent malaria but essential in the mosquito phase. *Proc Natl Acad Sci U S A.* 2015;112(33):10216-23. Epub 2015/04/02. doi: 10.1073/pnas.1423959112. PubMed PMID: 25831536; PMCID: PMC4547259.
30. Zhang T. Characterization and S-glutathionylation of hexokinase from the malaria parasite *Plasmodium falciparum*: Justus Liebig University; 2013.
31. Sakata-Kato T, Wirth DF. A Novel Methodology for Bioenergetic Analysis of *Plasmodium falciparum* Reveals a Glucose-Regulated Metabolic Shift and Enables Mode of Action Analyses of Mitochondrial Inhibitors. *ACS Infect Dis.* 2016;2(12):903-16. Epub 2016/10/11. doi: 10.1021/acsinfecdis.6b00101. PubMed PMID: 27718558; PMCID: PMC5518782.
32. Saliba KJ, Krishna S, Kirk K. Inhibition of hexose transport and abrogation of pH homeostasis in the intraerythrocytic malaria parasite by an O-3-hexose derivative. *FEBS Lett.* 2004;570(1-3):93-6. Epub 2004/07/15. doi: 10.1016/j.febslet.2004.06.032. PubMed PMID: 15251446.
33. Harris MT, Walker DM, Drew ME, Mitchell WG, Dao K, Schroeder CE, Flaherty DP, Weiner WS, Golden JE, Morris JC. Interrogating a hexokinase-selected small-molecule library for inhibitors of *Plasmodium falciparum* hexokinase. *Antimicrob Agents Chemother.* 2013;57(8):3731-7. Epub 2013/05/30. doi: 10.1128/AAC.00662-13. PubMed PMID: 23716053; PMCID: PMC3719756.